

Supplementary Materials: ShiftMorph: A Fast and Robust Convolutional Neural Network for 3D Deformable Medical Image Registration

Anonymous Authors

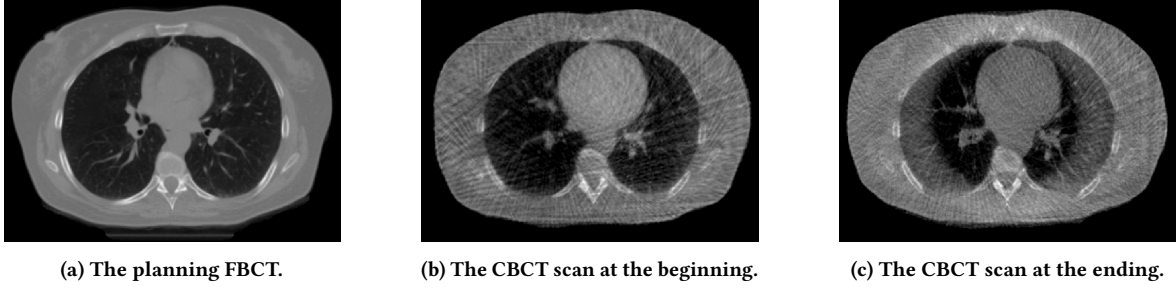


Figure 1: Example images from the ThoraxCBCT dataset.

1 WHY IS SHIFTMORPH ROBUST?

The shifted embedding module contributes to the main reason for robustness. This module produces eight different encoding results and averages them within groups, which is conducive to Gaussian noise removals. Expressly, the mean distribution of k samples from $N(0, \sigma^2)$ is $N(0, \frac{\sigma^2}{k})$. As a result, the energy of the noise can be significantly attenuated, stabilizing the output features and achieving good robustness. In the case of real noise with unknown structures, averaging can also suppress the feature variance to some extent, serving as a simple boosting method.

2 ROBUSTNESS TO REAL NOISE

We then use the ThoraxCBCT [1, 2] dataset to evaluate the robustness in the real-world noisy scenario, as well as the generalization ability. The ThoraxCBCT dataset is a benchmark for the registration problem of image-guided radiation therapy (IGRT) between pre-therapeutic fan-beam CT (FBCT) and interventional low-dose cone beam CT (CBCT) is addressed. The planning FBCT (inspiration) before therapy is of high quality, whereas the two corresponding

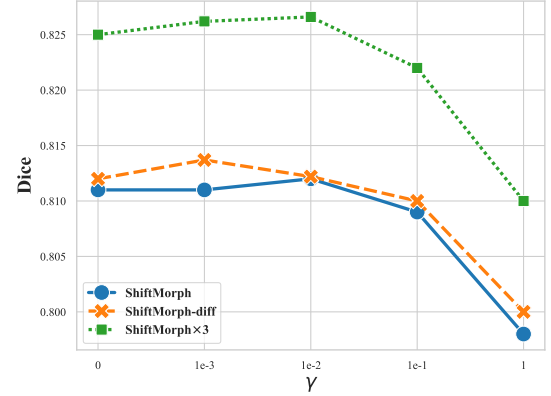


Figure 2: The impacts of the self-consistency learning on the OASIS dataset.

low-dose CBCT scans at the beginning and the end of therapy (expiration) contain noise with unknown complicated structures, as

Table 1: Robustness testing on the ThoraxCBCT dataset. The Dice score is computed using the binary masks.

	Training set				Validation set			
	Dice	TRE (mm)	TRE opt. (mm)	Folds (%)	Dice	TRE (mm)	TRE opt. (mm)	Folds (%)
TransMorph	0.6493 ⁸	22.22 ⁵	15.78 ⁵	19.14 ⁷	0.6005 ⁸	27.37 ⁷	20.18 ⁷	17.77 ⁷
TransMatch	0.6700 ⁷	19.37 ⁴	14.59 ⁴	14.67 ⁶	0.6176 ⁷	21.31 ⁴	16.01 ⁴	15.57 ⁶
VoxelMorph++	-	>30	>30	-	-	>30	>30	-
LapIRN	0.7043 ⁴	>30	>30	>30	0.6234 ⁶	>30	>30	>30
PCNet	0.6837 ⁶	24.37 ⁷	15.82 ⁶	0.4011 ³	0.6306 ⁵	26.43 ⁵	17.15 ⁵	0.3844 ³
FourierNet	0.7058 ⁵	24.33 ⁶	16.87 ⁷	0.0014 ¹	0.6565 ⁴	27.06 ⁶	18.82 ⁶	0.0036 ²
ShiftMorph	0.7132 ²	13.39 ¹	12.73 ¹	1.3576 ⁴	0.6785 ²	14.52 ¹	12.45 ²	1.1314 ⁴
ShiftMorph-diff	0.7111 ³	13.40 ²	12.70 ²	0.0015 ²	0.6759 ³	14.55 ²	12.44 ¹	0.0003 ¹
ShiftMorph $\times 3$	0.7542 ¹	17.02 ³	14.32 ³	4.5120 ⁵	0.7106 ¹	18.90 ³	14.71 ³	4.1390 ⁵

shown in Fig. 1. Similarly, the keypoint correspondences are automatically generated using corrfield. We then filter out the invalid values and use morphology operators to generate a mask for each scan. Only the training set (22 image pairs) and the validation set (6 image pairs) are available now.

We directly use the model weights trained in the Lung250M-4B dataset and assess how the registration performance degrades in this dataset. As evidenced by Tab.1, the proposed method performs the best in this challenging case. Comparingly, LapIRN and VoxelMorph++ cannot be generalized into this dataset, presenting abnormal deformation results.

3 PARAMETER SELECTION

The weight for the self-consistency loss, i.e. γ , is selected from a set of $\{0, 10^{-3}, 10^{-2}, 10^{-1}, 1\}$. As shown in Fig. 2, $\gamma = 0.01$ gives better dice scores for ShiftMorph and ShiftMorph $\times 3$. However, when applying the squaring and scaling skill, a smaller value, i.e., $\gamma = 0.001$, works better for ShiftMorph-diff. Higher γ will cause underfitting due to imposing too much regularization.

REFERENCES

- [1] Geoffrey D. Hugo, Elisabeth Weiss, William C. Sleeman, Salim Balik, Paul J. Keall, Jun Lu, and Jeffrey F. Williamson. 2016. Data from 4D Lung Imaging of NSCLC Patients (Version 2) [Data set]. <https://doi.org/10.7937/K9/TCIA.2016.ELN8YGLE>
- [2] Geoffrey D. Hugo, Elisabeth Weiss, William C. Sleeman, Salim Balik, Paul J. Keall, Jun Lu, and Jeffrey F. Williamson. 2017. A Longitudinal Four-Dimensional Computed Tomography and Cone Beam Computed Tomography Dataset for Image-Guided Radiation Therapy Research in Lung Cancer. *Medical Physics* 44, 2 (Feb. 2017), 762–771.